Integration of Massive MIMO and RIS to Serve Energy and Information Users

Mohammadali Mohammadi, Zahra Mobini, Hien Quoc Ngo, and Michail Matthaiou
Centre for Wireless Innovation (CWI), Queen's University Belfast, U.K.
Email:{m.mohammadi, zahra.mobini, hien.ngo, m.matthaiou}@qub.ac.uk

***Abstract*—We consider a reflecting intelligent surface (RIS)-assisted massive multiple-input multiple-output (MIMO) system to facilitate simultaneous wireless information and power transfer (SWIPT) towards two groups of information users (IUs) and energy users (EUs) over Rician fading channels. By considering partial zero-forcing (PZF) precoding at the base station (BS), we derive closed-from expressions for the achievable downlink spectral efficiency (SE) of the IUs and average harvested energy at the EUs. Our results rigorously demonstrate the impact of various system parameters on the actual performance. We next propose a max-min fairness transmit power allocation which seeks to maximize the minimum harvested power by EUs, subject to quality-of-service constraints at all IUs, relying on statistical channel state information (CSI) and a realistic non-linear energy harvesting (EH) model for the EUs. Our numerical results reveal that the interplay between the RIS and massive MIMO can significantly boost the performance of SWIPT in wireless networks.**

I. Introduction

Massive MIMO technology is regarded as a key technology for the fifth-generation (5G) and beyond wireless communication networks [1], [2], for its ability to provide very high quality of service for many users over the same time-frequency resources. Moreover, massive MIMO has been recognized as an effective countermeasure against the path-loss and scattering issues in SWIPT systems by steering radio-frequency (RF) energy beams towards users via simple signal processing techniques. Nevertheless, massive MIMO is still suffering from the blockage problem, which severely hinders seamless coverage provisioning in urban environments with dense obstacles. To overcome this challenge, a new developed technology termed as RISs [3], has been recently proposed for application in massive MIMO [4]–[6] and SWIPT systems [7]–[9]. A RIS consists of a large number of low-cost and energy efficient passive/semi-passive elements, which is regarded as a complementary architecture in wireless networks without the need to change their physical-layer standardization [3]. In principle, RISs can be flexibly deployed at proper locations to provide additional high-quality communication paths for IUs and/or EUs.

Despite the rich literature on RIS-assisted networks, only a few recent studies have investigated the application of RIS in massive MIMO systems from an information-theoretic point of view [4]–[6]. Particularly, in [4], the rate scaling order of an uplink (UL) RIS-aided multi-user massive MIMO system was studied under imperfect CSI. The authors in [5] analyzed and optimized the UL achievable rate in RIS-aided massive MIMO systems with statistical CSI. In [6], the impact of spatial correlation and interference on the achievable UL rate of RIS-aided massive MIMO systems was investigated and the problem of minimum user rate maximization was solved relying on the available statistical CSI. The deployment of RISs to assist in information/power transfer from a multi-antenna BS to multiple single-antenna IUs and EUs was recently studied in [9], [10]. Moreover, potential application scenarios of RIS-aided cell-free massive MIMO for SWIPT was discussed in [11]. However, none of these works have looked into the RIS-aided SWIPT massive MIMO systems. This motivates us to develop an analytical framework to characterize the interplay between the promising RIS technology and the existing massive MIMO technology in SWIPT systems. When SWIPT aims to achieve concurrent information and energy transmission efficiency for two groups of IUs and EUs, it is crucial to investigate the trade-off in allocating the available resources, such as power between the IUs and EUs.

To fill the above mentioned research gaps, in this paper, we study a RIS-aided SWIPT massive MIMO system with two groups of IUs and EUs. We aim to achieve a balanced performance between the concurrent information and energy transmission for a given spectrum and power budget. By applying the minimum mean square error (MMSE)-based method to estimate the aggregated BS-to-RIS-to-EU channels, we study the impact of pilot overhead, pilot contamination, and channel estimation errors on the SE and average harvested power at the system. The main technical contributions of this paper can be summarized as follows:

- We derive closed-form expressions for the achievable downlink (DL) SEs at the IUs and average harvested energy at the EUs, using PZF precoding at the BS. We consider statistical channel knowledge at the user's side, thus, our analytical results depend only on the location, angular information and Rician factors and hold for any finite number of antennas at the BS.
- We investigate the max-min fairness power allocation to maximize the minimum harvested power at the EUs, while the individual signal-to-noise-plus-interference ratio (SINR) requirements at all the IUs are satisfied. Numerical results show the benefit of the proposed power allocation in the finite medium to large number of antennas regime.

Notation: We use bold upper case letters to denote matrices, and lower case letters to denote vectors. The superscripts $(\cdot)^*$, $(\cdot)^T$ and $(\cdot)^H$ stand for the conjugate, transpose, and conjugate-

This project has received funding from the European Research Council (ERC) under the European Union's Horizon 2020 research and innovation programme (grant agreement No. 101001331).

transpose (Hermitian), respectively; $\mathbb{C}^{L\times N}$ denotes a $L \times N$ matrix; $\mathbf{I}_M$ and $\mathbf{0}_{M\times N}$ represent the $M \times M$ identity matrix and zero matrix of size $M \times N$, respectively; $\mathrm{tr}(\cdot)$ and $(\cdot)^{-1}$ denote the trace and the inverse operation; $\mathrm{diag}\{\cdot\}$ returns a diagonal matrix. A zero mean circular symmetric complex Gaussian distribution having variance σ^2 is denoted by $\mathcal{CN}(0, \sigma^2)$. Finally, $\mathbb{E}\{\cdot\}$ denotes the statistical expectation.

II. System Model

We consider a DL RIS-aided SWIPT massive MIMO system with K_I IUs and K_E EUs, cf. Figure 1. We focus on a special case where the direct link between the BS and EUs is unavailable due to severe blockage and a RIS, pre-deployed in the vicinity of the blocking object, is available to serve the blocked EUs [12]. We assume that the IUs are sufficiently far from the RIS and, thus, the reflected paths from RIS to the IUs are neglected. The BS and the RIS are equipped with M transmitting antennas and N reflecting elements, respectively, while all users are single-antenna devices. For notational simplicity, we define the sets $\mathcal{K}_\mathcal{I} = \{1, \ldots, K_I\}$ and $\mathcal{K}_\mathcal{E} = \{1, \ldots, K_E\}$ to collect the indices of the IUs and EUs, respectively. Moreover, the set of all RIS elements is denoted by $\mathcal{N} = \{1, \ldots, N\}$. We assume a quasi-static channel model, with each channel coherence interval (CCI) spanning τ_c time slots. In each CCI, the instantaneous channels from the BS-to-IUs, BS-to-RIS, and RIS-to-EUs are denoted by $\mathbf{H}_1 \in \mathbb{C}^{M\times K_I}$, $\mathbf{H}_2 \in \mathbb{C}^{M\times N}$, and $\mathbf{H}_3 \in \mathbb{C}^{N\times K_E}$, respectively. Then, the cascaded BS-RIS-EUs channel is $\mathbf{G} = \mathbf{H}_2\mathbf{\Theta}\mathbf{H}_3$, where $\mathbf{\Theta} = \mathrm{diag}\{e^{j\theta_1}, \ldots, e^{j\theta_N}\}$ is the RIS phase shift matrix and $\mathbf{G} = [\mathbf{g}_1, \ldots, \mathbf{g}_{K_E}]$, where $\mathbf{g}_\ell \in \mathbb{C}^{M\times 1}$ is the aggregate channel of EU $\ell \in \mathcal{K}_\mathcal{E}$.

Since IUs are located far away from the BS and rich scatterers are distributed on the ground, the channels between the BS and IUs are assumed to be Rayleigh faded as in [4]. In particular, $\mathbf{H}_1 = [\mathbf{h}_1, \ldots, \mathbf{h}_{K_I}]$, where $\mathbf{h}_k = \sqrt{\beta_{\mathtt{BI},k}}\tilde{\mathbf{h}}_k$ is the channel between the BS and IU $k \in \mathcal{K}_\mathcal{I}$ with large-scale fading coefficient $\beta_{\mathtt{BI},k}$ and small-scale fading vector $\tilde{\mathbf{h}}_k \in \mathbb{C}^{M\times 1}$ comprised of independent and identically distributed (i.i.d.) complex Gaussian random variables with zero-mean and unit variance. On the other hand, since the RIS is located is a high location (e.g., on the facade of a tall building in the proximity of the EUs), both line-of-sight (LoS) and non-line-of-sight (NLoS) transmission paths would exist in $\mathbf{H}_2$. Therefore, we model the BS-RIS channel by Rician fading, which is expressed as

$$\mathbf{H}_2 = \sqrt{\beta/(\delta+1)}\left(\sqrt{\delta}\bar{\mathbf{H}}_2 + \tilde{\mathbf{H}}_2\right), \tag{1}$$

where β is the path-loss factor, and δ is the Rician factor which represents the ratio between the power of the LoS component $\bar{\mathbf{H}}_2$ and the power of NLoS component $\tilde{\mathbf{H}}_2$, respectively. The elements of $\tilde{\mathbf{H}}_2$ are i.i.d. complex Gaussian random variables with zero mean and unit variance. We assume that the RIS is located closely to the EUs. This assumption is reasonable because, in general, RIS should be deployed near to the EUs to minimize path-loss. Since the RIS has a certain height and the distance between each EU and the RIS is short, the strength of the NLoS components is much weaker than that of the LoS components for the RIS-EU channels [4]. Accordingly, the RIS-EU channels are expected to be LoS-dominant. Therefore, the pure LoS RIS-EUs

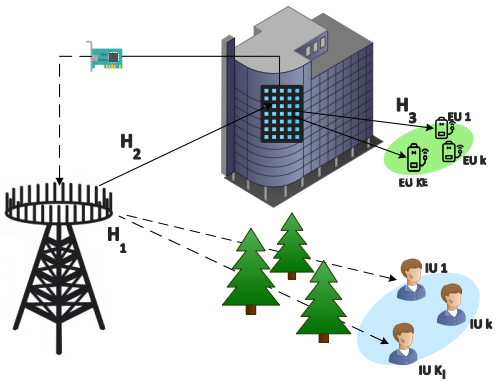

Fig. 1: RIS-assisted SWIPT massive MIMO system.

is assumed, and given by $\mathbf{H}_3 = [\sqrt{\beta_{\mathtt{rE},1}}\bar{\mathbf{f}}_1, \ldots, \sqrt{\beta_{\mathtt{rE},K_E}}\bar{\mathbf{f}}_{K_E}]$, where $\beta_{\mathtt{rE},\ell}$, $\forall \ell \in \mathcal{K}_\mathcal{E}$ is the path-loss for EU ℓ and $\bar{\mathbf{f}}_\ell \in \mathbb{C}^{N\times 1}$ is the deterministic LoS channel between the RIS and EU ℓ.

For LoS paths, the uniform linear array (ULA) and uniform squared planar array (USPA) models are adopted for the BS and the RIS, respectively [4], [13]. Then, the LoS components $\bar{\mathbf{f}}_\ell$ and $\bar{\mathbf{H}}_2$ are modeled

$$\begin{aligned}\bar{\mathbf{f}}_\ell &= \mathbf{a}_N(\phi^a_{\ell,t}, \phi^e_{\ell,t}),\ \forall \ell \in \mathcal{K}_\mathcal{E},\\ \bar{\mathbf{H}}_2 &= \mathbf{a}_M(\phi^a_r, \phi^e_r)\mathbf{a}^H_N(\phi^a_t, \phi^e_t),\end{aligned} \tag{2}$$

where $\phi^a_{\ell,t}$ and $\phi^e_{\ell,t}$ denote the azimuth and elevation angles of departure (AoD) from the RIS towards EU ℓ; ϕ^a_t and ϕ^e_t denote AoD from the BS towards RIS; ϕ^a_r and ϕ^e_r are the azimuth and elevation angles of arrivals (AoA) at the RIS from BS. Moreover, the q-th entry of the array response vector $\mathbf{a}_T(\vartheta^a, \vartheta^e) \in \mathbb{C}^{T\times 1}$, $T \in \{M, N\}$, is given by [6, Eq. (9)].

A. Channel Estimation

Since the RIS elements have no transmit RF chains, we consider a time-division duplexing (TDD) protocol for UL and DL transmissions and assume channel reciprocity for the CSI acquisition in the DL based on the UL training. Therefore, at the beginning of each CCI, τ time slots are used from the $K = |\mathcal{K}_\mathcal{I}| + |\mathcal{K}_\mathcal{E}|$ users to transmit the pilot signals to the BS. We termed these τ time slots as training phase. During the training phase, the cascaded channel BS-RIS-EUs and BS-IUs are estimated by the BS using pilot symbols from the users. To this end, the K users are assigned pilot sequences of length τ. Let $\mathbf{\Phi}_I = [\boldsymbol{\varphi}_1, \ldots, \boldsymbol{\varphi}_{K_I}]$ and $\mathbf{\Phi}_E = [\bar{\boldsymbol{\varphi}}_1, \ldots, \bar{\boldsymbol{\varphi}}_{K_E}]$, where $\sqrt{\tau}\boldsymbol{\varphi}_k \in \mathbb{C}^{\tau\times 1}$ ($\sqrt{\tau}\bar{\boldsymbol{\varphi}}_\ell \in \mathbb{C}^{\tau\times 1}$), with $\|\boldsymbol{\varphi}_k\|^2 = 1$ ($\|\bar{\boldsymbol{\varphi}}_\ell\|^2 = 1$), be the pilot sequence used by IU $k \in \mathcal{K}_\mathcal{I}$ (EU $\ell \in \mathcal{K}_\mathcal{E}$). We assume that $K < \tau$, meaning that some of the users can share the same orthogonal pilot sequences. The BS estimates the channels based on the received $M \times \tau$ pilot signal

$$\mathbf{Y}_p = \sqrt{\tau p}\mathbf{G}\mathbf{\Phi}^H_E + \sqrt{\tau p}\mathbf{H}_1\mathbf{\Phi}^H_I + \mathbf{N}, \tag{3}$$

where p is the common average transmission power of each user during the channel estimation stage, and $\mathbf{N}$ is the noise matrix whose elements are i.i.d. Gaussian variables following $\mathcal{CN}(0, \sigma^2_n)$. Then, the BS projects $\mathbf{Y}_p$ onto $\bar{\boldsymbol{\varphi}}_\ell$ ($\boldsymbol{\varphi}_k$) to estimate $\mathbf{g}_\ell$ ($\mathbf{h}_k$), by producing

$$\check{\mathbf{y}}_p = \sqrt{\tau p}\Big(\mathbf{g}_\ell + \sum_{k'\in\mathcal{K}_\mathcal{E}\setminus k}\mathbf{g}_{k'}\bar{\boldsymbol{\varphi}}^H_{k'}\bar{\boldsymbol{\varphi}}_\ell + \sum_{k''\in\mathcal{K}_\mathcal{I}}\mathbf{h}_{k''}\boldsymbol{\varphi}^H_{k''}\bar{\boldsymbol{\varphi}}_\ell\Big) + \mathbf{N}\bar{\boldsymbol{\varphi}}_\ell. \tag{4}$$

By invoking (1), the aggregate channel of the EU ℓ can be expressed as

$$\mathbf{g}_\ell = \sqrt{\lambda_\ell}\bar{\mathbf{H}}_2\boldsymbol{\Theta}\bar{\mathbf{f}}_\ell + \sqrt{\frac{\lambda_\ell}{\delta}}\tilde{\mathbf{H}}_2\boldsymbol{\Theta}\bar{\mathbf{f}}_\ell, \tag{5}$$

where $\lambda_\ell = \frac{\beta_{\mathrm{rE},\ell}\beta\delta}{\delta+1}$. It can be readily checked that, since $\tilde{\mathbf{H}}_2$ consists of i.i.d. $\mathcal{CN}(0,1)$ elements, the elements of vector $\tilde{\mathbf{H}}_2\boldsymbol{\Theta}\bar{\mathbf{f}}_\ell$ are linear combinations of independent Gaussian RVs, i.e., $\sqrt{\lambda_\ell}\tilde{\mathbf{H}}_2\boldsymbol{\Theta}\bar{\mathbf{f}}_\ell \sim \mathcal{CN}(\mathbf{0}, N\lambda_\ell\mathbf{I}_M)$. Therefore, $\mathbf{g}_\ell$ is a Gaussian vector with $\mathbf{g}_\ell \sim \mathcal{CN}\big(\sqrt{\lambda_\ell}\bar{\mathbf{H}}_2\boldsymbol{\Theta}\bar{\mathbf{f}}_\ell, N\lambda_\ell\mathbf{I}_M\big)$. Moreover, the received noise vector $\mathbf{N}\bar{\boldsymbol{\varphi}}_\ell \sim \mathcal{CN}(0,\sigma_n^2\mathbf{I}_M)$. Since the sum of independent Gaussian vectors is still a Gaussian vector, the observation vector for the channel of EU $\ell \in \mathcal{K}_\mathcal{E}$, in (4) is Gaussian distributed. Accordingly, we can apply MMSE estimator to obtain the channel estimate of $\mathbf{g}_k$. By invoking [14, Eq. (15.64)], the MMSE estimate of $\mathbf{g}_\ell$ is obtained as

$$\hat{\mathbf{g}}_\ell = \sqrt{\lambda_\ell}\bar{\mathbf{H}}_2\boldsymbol{\Theta}\bar{\mathbf{f}}_\ell + c_{g_\ell}\Big(\check{\mathbf{y}}_p - \sqrt{\lambda_\ell}\bar{\mathbf{H}}_2\boldsymbol{\Theta}\bar{\mathbf{f}}_\ell\Big),$$

where $c_{g_\ell} \triangleq \frac{\sqrt{\tau p}N\lambda_\ell}{\delta\sigma^2_{\check{\mathbf{w}}}}$, with $\sigma^2_{\check{\mathbf{w}}} = \tau p\big(\sum_{k'\in\mathcal{K}_\mathcal{E}} N\frac{\beta_{\mathrm{rE},k'}\beta}{\delta+1}|\bar{\boldsymbol{\varphi}}_{k'}^H\bar{\boldsymbol{\varphi}}_\ell|^2 + \sum_{k''\in\mathcal{K}_\mathcal{I}}\beta_{\mathtt{BI},k''}|\boldsymbol{\varphi}_{k''}^H\bar{\boldsymbol{\varphi}}_\ell|^2\big) + \sigma_n^2$. Moreover, by using a similar approach, the MMSE estimate of $\mathbf{h}_k$ can be obtained as $\hat{\mathbf{h}}_k = c_{h_k}\check{\mathbf{y}}_p$, where $c_{h_k} \triangleq \frac{\sqrt{\tau p}\beta_{\mathtt{BI},k}}{\sigma^2_{\check{\mathbf{v}}}}$ with $\sigma^2_{\check{\mathbf{v}}} = \tau p\big(\sum_{k'\in\mathcal{K}_\mathcal{I}}\beta_{\mathtt{BI},k'}|\boldsymbol{\varphi}_{k'}^H\boldsymbol{\varphi}_k|^2 + \sum_{k''\in\mathcal{K}_\mathcal{E}} N\frac{\beta_{\mathrm{rE},k''}\beta}{\delta+1}|\bar{\boldsymbol{\varphi}}_{k''}^H\boldsymbol{\varphi}_k|^2\big) + \sigma_n^2$. It is clear that the channel estimates are impaired by pilot contamination, which consists of interference from IUs/EUs using same pilot sequences as the IU/EU of interest in the training phase. We define the matrix of channel estimates for all users (IUs and EUs), as $\hat{\mathbf{H}} = [\hat{\mathbf{H}}_1, \hat{\mathbf{G}}] \in \mathbb{C}^{K\times M}$, where $\hat{\mathbf{H}}_1 = [\hat{\mathbf{h}}_1, \ldots, \hat{\mathbf{h}}_{K_I}]$ with $\hat{\mathbf{h}}_k \in \mathbb{C}^{M\times 1}$ and $\hat{\mathbf{G}} = [\hat{\mathbf{g}}_1, \ldots, \hat{\mathbf{g}}_{K_E}]$ with $\hat{\mathbf{g}}_\ell \in \mathbb{C}^{M\times 1}$.

The estimation error for the cascaded BS-RIS-EU link is given by $\tilde{\mathbf{g}}_\ell = \mathbf{g}_\ell - \hat{\mathbf{g}}_\ell$. The estimate and estimation error are independent and distributed as $\hat{\mathbf{g}}_\ell \sim \mathcal{CN}\Big(\sqrt{\lambda_\ell}\bar{\mathbf{H}}_2\boldsymbol{\Theta}\bar{\mathbf{f}}_\ell, \gamma_{\hat{g}_\ell}\mathbf{I}_M\Big)$ and $\tilde{\mathbf{g}}_\ell \sim \mathcal{CN}\Big(\mathbf{0}_{M\times 1}, (N\lambda_\ell - \gamma_{\hat{g}_\ell})\mathbf{I}_M\Big)$, respectively, where $\gamma_{\hat{g}_\ell} = \mathbb{E}\left\{|[\hat{\mathbf{g}}_\ell]_m|^2\right\}$ is the mean square of the estimate, given by

$$\gamma_{\hat{g}_\ell} = \left(\frac{\sqrt{\tau p}N\lambda_\ell}{\delta}\right)c_{g_\ell},\ \forall m = 1,\ldots,M. \tag{6}$$

Likewise, the estimation error for BS-IU link is given by $\tilde{\mathbf{h}}_k = \mathbf{h}_k - \hat{\mathbf{h}}_k$. The estimate and estimation error are independent and distributed as $\hat{\mathbf{h}}_k \sim \mathcal{CN}(\mathbf{0}_{M\times 1}, \gamma_{\hat{h}_k}\mathbf{I}_M)$ and $\tilde{\mathbf{h}}_k \sim \mathcal{CN}(\mathbf{0}_{M\times 1}, (\beta_{\mathtt{BI},k} - \gamma_{\hat{h}_k})\mathbf{I}_M)$, respectively, where $\gamma_{\hat{h}_k}$ is the mean square of the m-th channel estimate entry, given by

$$\gamma_{\hat{h}_k} = \mathbb{E}\left\{\left|\left[\hat{\mathbf{h}}_k\right]_m\right|^2\right\} = \sqrt{\tau p}\beta_{\mathtt{BI},k}c_{h_k},\ \forall m = 1,\ldots,M. \tag{7}$$

B. Signal Transmission

The channel estimates from UL training are used at the BS to generate precoding vectors for DL transmission. Let $\mathbf{W}_\mathrm{I} = [\mathbf{w}_{\mathrm{I},1}, \ldots, \mathbf{w}_{\mathrm{I},K_I}]$ and $\mathbf{W}_\mathrm{E} = [\mathbf{w}_{\mathrm{E},1}, \ldots, \mathbf{w}_{\mathrm{E},K_E}]$ denote the information and energy precoding matrix at the BS, respectively, where $\mathbf{w}_{\mathrm{I},k} \in \mathbb{C}^{M\times 1}$ and $\mathbf{w}_{\mathrm{E},\ell} \in \mathbb{C}^{M\times 1}$ are the precoding vector for IU k and EU ℓ, respectively, with $\mathbb{E}\{\|\mathbf{w}_{\mathrm{I},k}\|^2\} = 1$ and $\mathbb{E}\{\|\mathbf{w}_{\mathrm{E},\ell}\|^2\} = 1$. Moreover, denote by $\mathbf{x}_\mathrm{I} = [x_{\mathrm{I},1}, \ldots, x_{\mathrm{I},K_I}]^T$ and $\mathbf{x}_\mathrm{E} = [x_{\mathrm{E},1}, \ldots, x_{\mathrm{I},K_E}]^T$ the information and energy vector for IUs and EUs, while $x_{\mathrm{I},k}$ and $x_{\mathrm{E},\ell}$ are the information-carrying and energy-carrying signals for IU k and EU ℓ, respectively, satisfying $\mathbf{x}_\mathrm{I} \sim \mathcal{CN}(\mathbf{0}, \mathbf{I}_{K_I})$ and $\mathbf{x}_\mathrm{E} \sim \mathcal{CN}(\mathbf{0}, \mathbf{I}_{K_E})$ [4]. The transmit signal from the BS is given by $\mathbf{s} = \sum_{k\in\mathcal{K}_\mathcal{I}}\sqrt{\tilde{\rho}_{\mathrm{I},k}}\mathbf{w}_{\mathrm{I},k}x_{\mathrm{I},k} + \sum_{\ell\in\mathcal{K}_\mathcal{E}}\sqrt{\tilde{\rho}_{\mathrm{E},\ell}}\mathbf{w}_{\mathrm{E},\ell}x_{\mathrm{E},\ell}$, where $\tilde{\rho}_{\mathrm{I},k}$ and $\tilde{\rho}_{\mathrm{E},\ell}$ are the transmit powers for IU k and EU ℓ, respectively. The received signal at the IUs, $\mathbf{y}_\mathrm{I}$ and EUs, $\mathbf{y}_\mathrm{E}$, can be expressed as $\mathbf{y}_\mathrm{I} = \mathbf{G}^H\mathbf{s} + \mathbf{n}$, and $\mathbf{y}_\mathrm{E} = \mathbf{H}_1^H\mathbf{s} + \mathbf{z}$, respectively, where $\mathbf{n} \sim \mathcal{CN}(\mathbf{0}, \sigma_n^2\mathbf{I}_{K_I})$ and $\mathbf{z} \sim \mathcal{CN}(\mathbf{0}, \sigma_n^2\mathbf{I}_{K_E})$. Accordingly, the received data and energy signals at IU $k \in \mathcal{K}_\mathcal{I}$ and IU $\ell \in \mathcal{K}_\mathcal{E}$ can be written as

$$y_{\mathrm{I},k} = \sqrt{\rho_{\mathrm{I},k}}\mathbf{h}_k^H\mathbf{w}_{\mathrm{I},k}x_{\mathrm{I},k} + \sum_{t\in\mathcal{K}_\mathcal{I}\setminus k}\sqrt{\rho_{\mathrm{I},t}}\mathbf{h}_k^H\mathbf{w}_{\mathrm{I},t}x_{\mathrm{I},t} + \sum_{\ell\in\mathcal{K}_\mathcal{E}}\sqrt{\rho_{\mathrm{E},\ell}}\mathbf{h}_k^H\mathbf{w}_{\mathrm{E},\ell}x_{\mathrm{E},\ell} + \bar{n}_k, \tag{8}$$

$$y_{\mathrm{E},\ell} = \sum_{k\in\mathcal{K}_\mathcal{I}}\sqrt{\rho_{\mathrm{I},k}}\mathbf{g}_\ell^H\mathbf{w}_{\mathrm{I},k}x_{\mathrm{I},k} + \sum_{t\in\mathcal{K}_\mathcal{E}}\sqrt{\rho_{\mathrm{E},t}}\mathbf{g}_\ell^H\mathbf{w}_{\mathrm{E},t}x_{\mathrm{E},t} + \bar{z}_\ell, \tag{9}$$

where $\rho_{\mathrm{I},k} = \tilde{\rho}_{\mathrm{I},k}/\sigma_n^2$ and $\rho_{\mathrm{I},t} = \tilde{\rho}_{\mathrm{E},\ell}/\sigma_n^2$ are normalized signal-to-noise ratio (SNR) of data and energy symbols, respectively; $\bar{n}_k$ and $\bar{z}_\ell \sim \mathcal{CN}(0,1)$. We note that, to derive the harvested power at EU ℓ, we need to multiply the right hand side of (9) with the noise power, i.e., σ_n^2.

III. Beamforming Design and Performance Analysis

We evaluate the performance of the IUs in terms of DL SE in [bit/s/Hz] and the average of the harvested power at the EUs by applying PZF precoding at the BS.

A. Downlink Efficiency and Harvested RF Power

By invoking (8) and using the bounding technique in [1], known as the hardening bound, an achievable DL SE for IU k can be written as

$$\mathrm{SE}_k = \big(1 - \frac{\tau}{\tau_c}\big)\log_2(1 + \mathtt{SINR}_k) \qquad \text{[bit/s/Hz]}, \tag{10}$$

where the effective SINR is given by (11) at the top of the next page. The achievable DL SE in (10) is general and valid regardless of the precoding scheme used at the BS.

To characterize the harvested energy precisely, a non-linear EH model with the sigmoidal function is used. Therefore, the total harvested energy at EU ℓ is given by [10]

$$\Phi(\mathrm{E}_\ell) = \frac{\Omega(\mathrm{E}_\ell) - \phi\Lambda}{1 - \Lambda},\ \forall \ell \in \mathcal{K}_\mathcal{E}, \tag{12}$$

where ϕ is the maximum output DC power, $\Lambda = \frac{1}{1+\exp(ab)}$ is a constant to guarantee a zero input/output response, $\Omega(\mathrm{E}_\ell)$ is the traditional logistic function, given by

$$\Omega(\mathrm{E}_\ell) = \frac{\phi}{1 + \exp(-a(\mathrm{E}_\ell - b))}, \tag{13}$$

where a and b are constant related parameters that depend on the circuit. Moreover, E_ℓ denotes the received RF power at EU ℓ, $\forall \ell \in \mathcal{K}_\mathcal{E}$, which can be expressed as

$$\mathrm{E}_\ell = \eta\sigma_n^2\Big(\sum_{k\in\mathcal{K}_\mathcal{I}}\rho_{\mathrm{I},k}|\mathbf{g}_\ell^H\mathbf{w}_{\mathrm{I},k}|^2 + \sum_{t\in\mathcal{K}_\mathcal{E}}\rho_{\mathrm{E},t}|\mathbf{g}_\ell^H\mathbf{w}_{\mathrm{E},t}|^2 + 1\Big), \tag{14}$$

where $\eta \in (0,1]$ is the energy conversion efficiency. By inspecting the DL SE in (10) and the harvested energy in (14), we observe that the system performance depends on the precoding vectors adopted by the BS.

$$\mathtt{SINR}_k = \frac{\rho_{\mathrm{I},k}|\mathbb{E}\{\mathbf{h}_k^H\mathbf{w}_{\mathrm{I},k}\}|^2}{\sum_{t\in\mathcal{K}_\mathcal{I}}\rho_{\mathrm{I},t}\mathbb{E}\{|\mathbf{h}_k^H\mathbf{w}_{\mathrm{I},t}|^2\}+\sum_{\ell\in\mathcal{K}_\mathcal{E}}\rho_{\mathrm{E},\ell}\mathbb{E}\{|\mathbf{h}_k^H\mathbf{w}_{\mathrm{E},\ell}|^2\}-\rho_{\mathrm{I},k}|\mathbb{E}\{\mathbf{h}_k^H\mathbf{w}_{\mathrm{I},k}\}|^2+1}. \tag{11}$$

B. Partial Zero-Forcing Precoding

In massive MIMO, ZF is nearly optimal for data transmission, while maximum ratio transmission (MRT) guarantees the maximum harvested energy for the EUs. Thus, we propose to use the PZF precoding where the BS transmits to the IUs with full ZF and to the EUs with MRT. The signal sent by the BS employing PZF, is thus given by $\mathbf{s} = \sum_{k\in\mathcal{K}_\mathcal{I}}\sqrt{\rho_{\mathrm{I},k}}\mathbf{w}_{\mathrm{I},k}^{\mathtt{PZF}}x_{\mathrm{I},k} + \sum_{\ell\in\mathcal{K}_\mathcal{E}}\sqrt{\rho_{\mathrm{E},\ell}}\mathbf{w}_{\mathrm{E},\ell}^{\mathtt{MRT}}x_{\mathrm{E},\ell}$, with

$$\mathbf{w}_{\mathrm{I},k}^{\mathtt{PZF}} = \alpha_{\mathtt{PZF},k}\hat{\mathbf{H}}_1(\hat{\mathbf{H}}_1^H\hat{\mathbf{H}}_1)^{-1}\mathbf{e}_k^I, \tag{15a}$$

$$\mathbf{w}_{\mathrm{E},\ell}^{\mathtt{MRT}} = \alpha_{\mathtt{MRT},\ell}\hat{\mathbf{G}}\mathbf{e}_\ell^E, \tag{15b}$$

where $\mathbf{e}_k^I$ ($\mathbf{e}_\ell^E$) is the k-th column of $\mathbf{I}_{K_I}$ (ℓ-th column of $\mathbf{I}_{K_E}$). Moreover, $\alpha_{\mathtt{PZF},k} = \frac{1}{\sqrt{\mathbb{E}\{\|\hat{\mathbf{H}}_1(\hat{\mathbf{H}}_1^H\hat{\mathbf{H}}_1)^{-1}\mathbf{e}_k^I\|^2\}}}$ and $\alpha_{\mathtt{MRT},\ell} = \frac{1}{\sqrt{\mathbb{E}\{\|\hat{\mathbf{G}}\mathbf{e}_\ell^E\|^2\}}}$ denote the precoding normalization factors and are obtained as follows. Let $\tau_{\mathcal{K}_\mathcal{I}} \leq \tau$ be the number of different pilots used by IUs. Assuming Rayleigh fading for BS-IU links, the expectation term in $\alpha_{\mathtt{PZF},k}$ is obtained as

$$\mathbb{E}\Big\{\Big\|\hat{\mathbf{H}}_1(\hat{\mathbf{H}}_1^H\hat{\mathbf{H}}_1)^{-1}\mathbf{e}_k^I\Big\|^2\Big\} = \mathbb{E}\Big\{\Big[\Big(\hat{\mathbf{H}}_1^H\hat{\mathbf{H}}_1\Big)^{-1}\Big]_{k,k}\Big\}$$
$$= \frac{1}{\gamma_{\hat{h}_k}\tau_{\mathcal{K}_\mathcal{I}}}\mathbb{E}\Big\{\mathrm{tr}(\mathbf{X}^{-1})\Big\} = \frac{1}{(M-\tau_{\mathcal{K}_\mathcal{I}})\gamma_{\hat{h}_k}}, \tag{16}$$

where $\mathbf{X}$ is a $\tau_{\mathcal{K}_\mathcal{I}}\times\tau_{\mathcal{K}_\mathcal{I}}$ central Wishart matrix with M degrees of freedom, satisfying $M \geq \tau_{\mathcal{K}_\mathcal{I}}+1$, and covariance matrix $\mathbf{I}_{\tau_{\mathcal{K}_\mathcal{I}}}$, while the last equality is obtained by using [15, Lemma 2.10]. We note that if all the IUs are assigned mutually orthogonal pilots, then $\tau_{\mathcal{K}_\mathcal{I}} = K_I$. Moreover, for $\alpha_{\mathtt{MRT},\ell}$ we obtain

$$\mathbb{E}\Big\{\big\|\hat{\mathbf{G}}\mathbf{e}_\ell^E\big\|^2\Big\} = \mathbb{E}\Big\{\big\|\hat{\mathbf{g}}_\ell\big\|^2\Big\} = M\big(\gamma_{\hat{g}_\ell} + \lambda_\ell\Xi_{\ell,\ell}(\boldsymbol{\Theta})\big),$$

where $\Xi_{\ell,t}(\boldsymbol{\Theta}) \triangleq \bar{\mathbf{f}}_\ell^H\boldsymbol{\Theta}^H\mathbf{a}_N\mathbf{a}_N^H\boldsymbol{\Theta}\bar{\mathbf{f}}_t$ and we have used the fact that $\hat{\mathbf{g}}_\ell \sim \mathcal{CN}\big(\sqrt{\lambda_\ell}\bar{\mathbf{H}}_2\boldsymbol{\Theta}\bar{\mathbf{f}}_\ell, \gamma_{\hat{g}_\ell}\mathbf{I}_M\big)$.

Theorem 1. *The ergodic SE for the k-th IU, achieved by PZF scheme is given in closed-form by* (10)*, where the effective SINR is given by* (17) *at the top of the next page, while $\mathcal{P}_k \subset \mathcal{K}_\mathcal{I}$ is the set of IUs' indices share the same pilot with IU k.*

Proof. See Appendix A. □

Theorem 2. *With the PZF scheme, the expected energy harvested by the EU $\ell \in \mathcal{K}_\mathcal{E}$, is given by*

$$Q_\ell = (\tau_c-\tau)\sigma_n^2\Big(\frac{\beta_{\mathtt{rE},\ell}\beta}{\delta+1}\Big(N+\delta\Xi_{\ell,\ell}(\boldsymbol{\Theta})\Big)\Big(\sum_{k\in\mathcal{K}_\mathcal{I}}\rho_{\mathrm{I},k}\Big)$$
$$+\sum_{t\in\mathcal{K}_\mathcal{E}\setminus\{\mathcal{S}_\ell\}}\rho_{\mathrm{E},t}\alpha_{\mathtt{MRT},t}^2\Psi_1(\boldsymbol{\Theta})+\sum_{\ell'\in\mathcal{S}_\ell}\rho_{\mathrm{E},\ell'}\alpha_{\mathtt{MRT},\ell}^2\Psi_2(\boldsymbol{\Theta})+1\Big), \tag{18}$$

where $\mathcal{S}_\ell \subset \mathcal{K}_\mathcal{E}$ is the set of EUs' indices that share the same pilot with EU ℓ and

$$\Psi_1(\boldsymbol{\Theta}) = M\lambda_\ell\Big(\gamma_{\hat{g}_t}\Xi_{\ell,\ell}(\boldsymbol{\Theta}) + M\lambda_t|\Xi_{\ell,t}(\boldsymbol{\Theta})|^2$$
$$+\frac{N}{\delta}\gamma_{\hat{g}_t} + N\lambda_t\Xi_{t,t}(\boldsymbol{\Theta})\Big)$$
$$\Psi_2(\boldsymbol{\Theta}) = M(M+1)\gamma_{\hat{g}_\ell}^2 + M\lambda_\ell\Xi_{\ell,\ell}(\boldsymbol{\Theta})$$
$$\times\big(2(M+1)\gamma_{\hat{g}_\ell} + M\lambda_\ell\Xi_{\ell,\ell}(\boldsymbol{\Theta})\big). \tag{19}$$

Proof. See Appendix B. □

Remark 1. *To gain further insights into the harvested energy, we look into the case where the BS-RIS channel reduces to a Rayleigh fading channel containing only NLoS paths, i.e., $\delta \to 0$. Then, the average harvested energy at EU ℓ, is*

$$Q_\ell^{\mathtt{NLOS}} = (\tau_c-\tau)\sigma_n^2\Big(N\beta_{\mathtt{rE},\ell}\beta\Big(\sum_{k\in\mathcal{K}_\mathcal{I}}\rho_{\mathrm{I},k}+\sum_{t\in\mathcal{K}_\mathcal{E}}\rho_{\mathrm{E},t}\Big)$$
$$+M\sum_{\ell'\in\{\mathcal{S}_\ell\}}\rho_{\mathrm{E},\ell'}\gamma_{\hat{g}_\ell}^{\mathtt{NLOS}}+1\Big), \tag{20}$$

where $\gamma_{\hat{g}_\ell}^{\mathtt{NLOS}}$ is $\gamma_{\hat{g}_\ell}$ obtained at $\delta = 0$.

IV. Optimum Power Allocation Design

By exploiting the closed-form expressions for the average harvested energy and SE, we aim to maximize the minimum harvested power by EUs subject to the transmit power constraint at the BS, i.e., $\tilde{\rho}$ and individual SINR constraints at different IUs, given by γ_k, $k \in \mathcal{K}_\mathcal{I}$, i.e.,[1]

$$(\mathrm{P}_1): \max_{\boldsymbol{\rho}} \quad \min_{\ell} \ \mathbb{E}\left\{\Phi\left(\mathrm{E}_\ell(\boldsymbol{\rho})\right)\right\}, \tag{21a}$$

$$\text{s.t.} \quad \mathrm{SINR}_k(\boldsymbol{\rho}) \geq \gamma_k, \ \forall k \in \mathcal{K}_\mathcal{I}, \tag{21b}$$

$$\sum_{k\in\mathcal{K}_\mathcal{I}}\tilde{\rho}_{\mathrm{I},k} + \sum_{\ell\in\mathcal{K}_\mathcal{E}}\tilde{\rho}_{\mathrm{E},\ell} \leq \tilde{\rho}, \tag{21c}$$

where $\boldsymbol{\rho} = [\rho_{\mathrm{I},1},\ldots,\rho_{\mathrm{I},K_I},\rho_{\mathrm{E},1},\ldots,\rho_{\mathrm{E},K_E}]$. By inspecting (12), we notice that Λ does not have any effect on the the optimization problem. Therefore, we directly consider $\Omega(\mathrm{E}_\ell)$ to describe the harvested energy at EU ℓ. In order to facilitate the derivations, we first introduce the auxiliary variable t, and reformulate problem (P_1) as

$$(\mathrm{P}_2): \max_{\boldsymbol{\rho},t} \quad t \tag{22a}$$

$$\text{s.t.} \quad \mathbb{E}\left\{\Omega\left(\mathrm{E}_\ell(\boldsymbol{\rho})\right)\right\} \geq t, \quad \forall\ell \in \mathcal{K}_\mathcal{E}, \tag{22b}$$

$$(21\text{b}),\ (21\text{c}). \tag{22c}$$

Since the logistic function in (13) is a convex function of E_ℓ, by applying Jensen's inequality, we have $\mathbb{E}\left\{\Omega\left(\mathrm{E}_\ell(\boldsymbol{\rho})\right)\right\} \geq \Omega\left(\mathbb{E}\left\{\mathrm{E}_\ell(\boldsymbol{\rho})\right\}\right) = \Omega\left(Q_\ell(\boldsymbol{\rho})\right)$. The inverse function of (13), can be written as $E_\ell(\Omega) = b - \frac{1}{a}\ln\Big(\frac{\phi-\Omega}{\Omega}\Big), \forall\ell$. Therefore, by utilizing $E_\ell(\Omega)$, we replace the left hand side of (22b) by its lower bound as

$$(\mathrm{P}_3): \max_{\boldsymbol{\rho},t} \quad t \tag{23a}$$

$$\text{s.t.} \quad Q_\ell\left(\boldsymbol{\rho}\right) \geq b - \frac{1}{a}\ln\Big(\frac{\phi-t}{t}\Big), \ \forall\ell, \tag{23b}$$

$$(21\text{b}),\ (21\text{c}). \tag{23c}$$

The constraints (23b) are non-convex. In the following, we propose to use the successive convex approximation (SCA) to transform the non-convex constraints to convex approximation expressions. By applying a first-order Taylor approximation, constraint (23b) can be written as

$$Q_\ell\left(\boldsymbol{\rho}\right) \geq \ \Big(b - \frac{1}{a}\ln\Big(\frac{\phi-t^{(r)}}{t^{(r)}}\Big)\Big) + \frac{\phi\big(t-t^{(r)}\big)}{at^{(r)}\big(\phi-t^{(r)}\big)}, \tag{24}$$

[1] In general, the system performance will improve if the phase shift at the RIS is also optimized. However, in this work, we assume the phase shift is predesigned, and focus on power allocation to control the near-far effect of different users' locations and requirements. The joint power and phase shift control is interesting and left for future work.

$$\mathrm{SINR}_k^{\mathrm{PZF}} = \frac{(M-\tau_{\mathcal{K}_\mathcal{I}})\rho_{\mathrm{I},k}\gamma_{\hat{h}_k}}{\sum_{t\in\mathcal{P}_k\setminus\{k\}}(M-\tau_{\mathcal{K}_\mathcal{I}})\rho_{\mathrm{I},t}\gamma_{\hat{h}_k}+\sum_{t\in\mathcal{K}_\mathcal{I}\setminus\mathcal{P}_k}\rho_{\mathrm{I},t}(\beta_{\mathtt{BI},k}-\gamma_{\hat{h}_k})+\sum_{\ell\in\mathcal{K}_\mathcal{E}}\rho_{\mathrm{E},\ell}\beta_{\mathtt{BI},k}+1}, \tag{17}$$

Algorithm 1 Solving Problem (21)

1: **Initialize**: $n=0$, and $t^{(0)}$.
2: **repeat**
3: Update $n=n+1$.
4: Solve (25) to obtain its optimal solution t^*.
5: Update $t^{(n)}=t^*$.
6: **until** convergence

where $t^{(r)}$ is the value of the variable t after the r-th iteration in the proposed SCA-based algorithm. Thus, given the optimized values from the r-th iteration, the original problem (P_1) can be approximately transformed at the $(r+1)$-th iteration to

$$(\mathrm{P}_4): \max_{\boldsymbol{\rho},t} \quad t \tag{25a}$$

$$\text{s.t.} \quad (21b),\ (21c),\ (24). \tag{25b}$$

To this end, we propose an SCA-based algorithm to solve the power allocation problem in **Algorithm 1**.

V. Numerical Results

In this section, we verify the correctness of our derived results and the performance of the proposed power allocation algorithm. The distance-dependent path-loss model from [13] is used, where the large-scale coefficients are modeled as $L(d) = C_0\big(d/d_0\big)^{-\kappa}, L \in \{\beta_{\mathtt{BI},k}, \beta_{\mathtt{rE},\ell}, \beta\}$, where $d \in \{d_{\mathtt{B,IU_k}}, d_{\mathtt{I,EU}_\ell}, d_{\mathtt{I,BI}}\}$, with $d_{\mathtt{B,IU_k}}$, $d_{\mathtt{I,EU}_\ell}$, and $d_{\mathtt{I,BI}}$ are the distances between the BS and IU $k \in \mathcal{K}_\mathcal{I}$, the RIS and EU $\ell \in \mathcal{K}_\mathcal{E}$, and the BS and RIS, respectively; C_0 is the path-loss at the reference distance $d_0 = 1$ m and κ denotes the path-loss exponent. Here, we assume $C_0 = -30$ dB and the path-loss exponents of the BS-RIS link, RIS-EU link, and BS-IU link are set as $\kappa_{\mathtt{BI}} = 2.2$, $\kappa_{\mathtt{B,IU_k}} = 3.5$, and $\kappa_{\mathtt{I,EU}_\ell} = 2.8$ [13]. Unless otherwise stated, we set $\eta = 0.8$, $\tau_c = 196$, $\delta = 3$ dB, and $\tau = 10$ symbols are utilized for channel estimation. The transmit power of the pilot signal for each user is $p = 25$ dBm, transmit power of BS is 40 dBm, and the noise power is $\sigma_n^2 = -94$ dBm The non-linear EH parameters are set as $a = 2400$ $\frac{1}{\text{Watt}}$, $b = 0.003$ Watt, and $\phi = 0.02$ Watt [10]. The convergence tolerance of the proposed algorithms is set to 10^{-4}.

Figure 2 shows the per-EU average harvested power as a function of BS antenna number and for different number of RIS elements. A discrete Fourier transform (DFT) matrix and random phase shift (Rnd) are considered for the RIS reflecting elements. We point out that due to blockage, there is no direct link between the EUs and BS, thus, without the use of RIS, the average harvested power at the EUs is 0 Watt. On the other hand, by deploying the RIS at a proper location (to provide LOS transmission paths between the BS and RIS), the RIS can cover the entire blockage area and provide large amount of power for the EUs. It is clear that by increasing the number of RIS elements, the gap between the performance of the Rician and Rayleigh cases (for the $\mathbf{H}_2$ channel) is reduced as more scattered waves can be steered towards the EUs.

In Figure 3, the effectiveness of the proposed power allocation at the BS (OPA) over the equal power allocation (EPA) for

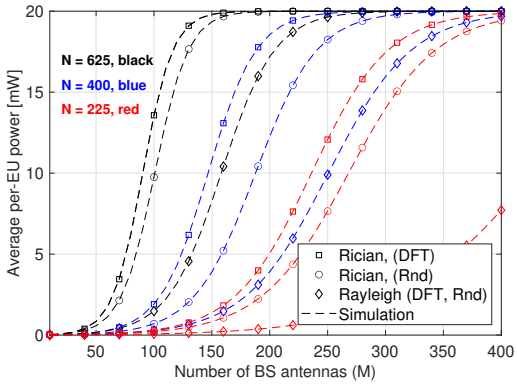

Fig. 2: Average harvested power ($K_I = 5$, $K_E = 3$).

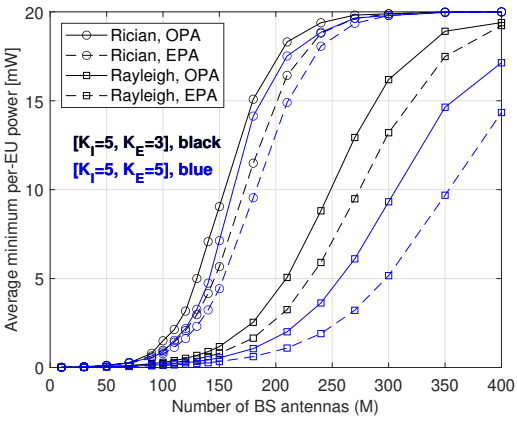

Fig. 3: Average minimum per-UE harvested power with equal and optimal power allocation ($N = 400$).

$N = 400$ and two different number of $[K_I, K_E]$ setups is presented. It is clear that the minimum per-EU harvested power is significantly increased, especially when the number of BS antennas is increased. Moreover, we observe that by increasing the number of EUs, the minimum per-EU power is decreased, while the total amount of harvested power by all the EUs increases.

VI. Conclusion

We studied the performance of RIS-assisted massive MIMO SWIPT systems with statistical CSI and in the presence of channel estimation errors. By leveraging on new closed-form SE and average harvested power expressions, a max-min power allocation policy was proposed that maximized the smallest harvested energy of all the EUs and ensures a pre-determined quality of service for IUs. We show that our proposed power allocation algorithm can achieve up to 47% gain over the equal power allocation and for specific system setup.

Appendix A
Proof of Theorem 1

By plugging $\mathbf{w}_{\mathrm{I},k}^{\mathrm{PZF}}$ into (11) and exploiting the independence between the channel estimation errors and the estimates, the numerator can be obtained as

$$\mathbb{E}\{\mathbf{h}_k^H\mathbf{w}_{\mathrm{I},k}^{\mathrm{PZF}}\} = \mathbb{E}\{(\hat{\mathbf{h}}_k^H+\tilde{\mathbf{h}}_k^H)\mathbf{w}_{\mathrm{I},k}^{\mathrm{PZF}}\} = \sqrt{(M-\tau_{\mathcal{K}_\mathcal{I}})\gamma_{\hat{h}_k}}, \tag{26}$$

$$Q_\ell \overset{(a)}{=} (\tau_c-\tau)\sigma_n^2\Bigg(\sum_{k\in\mathcal{K}_\mathcal{I}}\rho_{\mathrm{I},k}\mathbb{E}\left\{\mathbf{g}_\ell^H\mathbb{E}\{\mathbf{w}_{\mathrm{I},k}^{\mathtt{PZF}}(\mathbf{w}_{\mathrm{I},k}^{\mathtt{PZF}})^H\}\mathbf{g}_\ell\right\}+\sum_{t\in\mathcal{K}_\mathcal{E}\setminus\{\mathcal{S}_\ell\}}\rho_{\mathrm{E},t}\mathbb{E}\left\{\mathbf{g}_\ell^H\mathbb{E}\left\{\mathbf{w}_{\mathrm{E},t}^{\mathtt{MRT}}(\mathbf{w}_{\mathrm{E},t}^{\mathtt{MRT}})^H\right\}\mathbf{g}_\ell\right\}$$
$$+\sum_{\ell'\in\mathcal{S}_\ell}\rho_{\mathrm{E},\ell'}\mathbb{E}\left\{\left|(\hat{\mathbf{g}}_\ell^H+\tilde{\mathbf{g}}_\ell^H)\mathbf{w}_{\mathrm{E},\ell'}^{\mathtt{MRT}}\right|^2\right\}+1\Bigg) \tag{29}$$
$$\overset{(b)}{\approx}(\tau_c-\tau)\sigma_n^2\Bigg(\frac{\beta_{\mathtt{rE},\ell}\beta}{\delta+1}\Big(N+\delta\Xi_{\ell,\ell}(\mathbf{\Theta})\Big)\Big(\sum_{k\in\mathcal{K}_\mathcal{I}}\rho_{\mathrm{I},k}\Big)+\sum_{t\in\mathcal{K}_\mathcal{E}\setminus\{\mathcal{S}_\ell\}}\rho_{\mathrm{E},t}\alpha^2_{\mathtt{MRT},t}\mathbb{E}\left\{\mathbf{g}_\ell^H\mathbb{E}\left\{\hat{\mathbf{g}}_t(\hat{\mathbf{g}}_t)^H\right\}\mathbf{g}_\ell\right\}+\sum_{\ell'\in\mathcal{S}_\ell}\rho_{\mathrm{E},\ell'}\alpha^2_{\mathtt{MRT},\ell}\mathbb{E}\left\{\left\|\hat{\mathbf{g}}_\ell\right\|^4\right\}+1\Bigg),$$

where we used the fact that $\tilde{\mathbf{h}}_k$ is a zero-mean random vector.

The first term of the denominator in (11), can be derived as

$$\sum_{t\in\mathcal{K}_\mathcal{I}}\rho_{\mathrm{I},t}\mathbb{E}\{|\mathbf{h}_k^H\mathbf{w}_{\mathrm{I},t}^{\mathtt{PZF}}|^2\}=\sum_{t\in\mathcal{K}_\mathcal{I}}\rho_{\mathrm{I},t}\mathbb{E}\{|(\hat{\mathbf{h}}_k^H+\tilde{\mathbf{h}}_k^H)\mathbf{w}_{\mathrm{I},t}^{\mathtt{PZF}}|^2\}$$
$$\overset{(a)}{=}\sum_{t\in\mathcal{P}_k}\rho_{\mathrm{I},t}\mathbb{E}\{|\hat{\mathbf{h}}_k^H\mathbf{w}_{\mathrm{I},t}^{\mathtt{PZF}}|^2\}+\sum_{t\in\mathcal{K}_\mathcal{I}}\rho_{\mathrm{I},t}\mathbb{E}\{|\tilde{\mathbf{h}}_k^H\mathbf{w}_{\mathrm{I},t}^{\mathtt{PZF}}|^2\}$$
$$\overset{(b)}{=}\sum_{t\in\mathcal{P}_k}(M-\tau_{\mathcal{K}_\mathcal{I}})\rho_{\mathrm{I},t}\gamma_{\hat{h}_k}+\sum_{t\in\mathcal{K}_\mathcal{I}}\rho_{\mathrm{I},t}(\beta_{\mathtt{BI},k}-\gamma_{\hat{h}_k}), \tag{27}$$

where we have exploited: in (a) $\hat{\mathbf{h}}_k^H\mathbf{w}_{\mathrm{I},t}^{\mathtt{PZF}}=0$, $t\neq k$ and $t\notin\mathcal{P}_k$; in (b) $\tilde{\mathbf{h}}_k$ is independent of $\mathbf{w}_{\mathrm{I},t}^{\mathtt{PZF}}$. To derive the second term in (11), by exploiting the independence between $\mathbf{h}_k$ and $\mathbf{w}_{\mathrm{E},\ell}^{\mathtt{MRT}}$, we obtain $\mathbb{E}\{|\mathbf{h}_k^H\mathbf{w}_{\mathrm{E},\ell}^{\mathtt{MRT}}|^2\}$ as

$$\mathbb{E}\{\mathbf{h}_k^H\mathbb{E}\{\mathbf{w}_{\mathrm{E},\ell}^{\mathtt{MRT}}(\mathbf{w}_{\mathrm{E},\ell}^{\mathtt{MRT}})^H\}\mathbf{h}_k\}=\beta_{\mathtt{BI},k}. \tag{28}$$

To this end, by substituting (26), (27), and (28) into (11), the desired result in (17) is obtained.

Appendix B
Proof of Theorem 2

By invoking (14), $Q_\ell=(\tau_c-\tau)\sigma_n^2\mathbb{E}\{\mathrm{E}_\ell\}$ can be expressed as (29) at the top of the page, where we have exploited: in (a) $\mathbf{g}_\ell$ is independent of $\mathbf{w}_{\mathrm{I},k}^{\mathtt{PZF}}$ ($\forall k$) and $\mathbf{w}_{\mathrm{E},t}^{\mathtt{MRT}}$ for $t\in\mathcal{K}_\mathcal{E}\setminus\{\mathcal{S}_\ell\}$; in (b) cross-expectations are vanished as $\tilde{\mathbf{g}}_\ell$ is zero-mean vector and independent of $\mathbf{w}_{\mathrm{E},\ell'}^{\mathtt{MRT}}$ and approximation is due to neglecting harvested power from channel estimation error at the last term. To this end, by using Lemma 1, and then applying $\mathbb{E}\{\tilde{\mathbf{x}}^H\mathbf{A}\tilde{\mathbf{x}}\}=\boldsymbol{\mu}^H\mathbf{A}\boldsymbol{\mu}+\mathrm{tr}(\mathbf{A}\mathbf{\Sigma})$ for $\tilde{\mathbf{x}}\sim\mathcal{CN}(\boldsymbol{\mu}_{n\times1},\mathbf{\Sigma})$ and a positive definite Hermitian matrix $\mathbf{A}$, the desired result in (18) is obtained.

Lemma 1. *For a non-zero mean Gaussian vector* $\hat{\mathbf{g}}_\ell\sim\mathcal{CN}\big(\sqrt{\lambda_\ell}\bar{\mathbf{H}}_2\mathbf{\Theta}\bar{\mathbf{f}}_\ell,\gamma_{\hat{g}_\ell}\mathbf{I}_M\big)$*, we have* $\mathbb{E}\left\{\|\hat{\mathbf{g}}_\ell\|^4\right\}=\Psi_2(\mathbf{\Theta})$*, where* $\Psi_2(\mathbf{\Theta})$ *has been given in* (19)*.*

Proof. Let us define $\hat{\mathbf{g}}_\ell=\tilde{\hat{\mathbf{g}}}_\ell+\bar{\hat{\mathbf{g}}}_\ell$, where $\mathbb{E}\{\tilde{\hat{\mathbf{g}}}_\ell\}=\mathbf{0}_{M\times1}$. Therefore, we have

$$\mathbb{E}\{\,\|\hat{\mathbf{g}}_\ell\|^4\,\}=A_1+A_2+A_3+A_4, \tag{31}$$

where, by ignoring the zero cross-expectations, we have

$$A_1=\mathbb{E}\big\{(\tilde{\hat{\mathbf{g}}}_\ell^H\tilde{\hat{\mathbf{g}}}_\ell\tilde{\hat{\mathbf{g}}}_\ell^H\tilde{\hat{\mathbf{g}}}_\ell+\tilde{\hat{\mathbf{g}}}_\ell^H\tilde{\hat{\mathbf{g}}}_\ell\bar{\hat{\mathbf{g}}}_\ell^H\tilde{\hat{\mathbf{g}}}_\ell+\tilde{\hat{\mathbf{g}}}_\ell^H\bar{\hat{\mathbf{g}}}_\ell\tilde{\hat{\mathbf{g}}}_\ell^H\tilde{\hat{\mathbf{g}}}_\ell+\bar{\hat{\mathbf{g}}}_\ell^H\tilde{\hat{\mathbf{g}}}_\ell\bar{\hat{\mathbf{g}}}_\ell^H\tilde{\hat{\mathbf{g}}}_\ell)\big\}$$
$$A_2=\mathbb{E}\big\{\left(\tilde{\hat{\mathbf{g}}}_\ell^H\bar{\hat{\mathbf{g}}}_\ell\tilde{\hat{\mathbf{g}}}_\ell^H\tilde{\hat{\mathbf{g}}}_\ell+\tilde{\hat{\mathbf{g}}}_\ell^H\bar{\hat{\mathbf{g}}}_\ell\bar{\hat{\mathbf{g}}}_\ell^H\tilde{\hat{\mathbf{g}}}_\ell+\tilde{\hat{\mathbf{g}}}_\ell^H\bar{\hat{\mathbf{g}}}_\ell\tilde{\hat{\mathbf{g}}}_\ell^H\bar{\hat{\mathbf{g}}}_\ell\right)\big\}$$
$$A_3=\mathbb{E}\big\{\left(\bar{\hat{\mathbf{g}}}_\ell^H\tilde{\hat{\mathbf{g}}}_\ell\tilde{\hat{\mathbf{g}}}_\ell^H\tilde{\hat{\mathbf{g}}}_\ell+\bar{\hat{\mathbf{g}}}_\ell^H\tilde{\hat{\mathbf{g}}}_\ell\bar{\hat{\mathbf{g}}}_\ell^H\tilde{\hat{\mathbf{g}}}_\ell+\bar{\hat{\mathbf{g}}}_\ell^H\tilde{\hat{\mathbf{g}}}_\ell\tilde{\hat{\mathbf{g}}}_\ell^H\bar{\hat{\mathbf{g}}}_\ell\right)\big\}$$
$$A_4=\mathbb{E}\big\{\left(\bar{\hat{\mathbf{g}}}_\ell^H\bar{\hat{\mathbf{g}}}_\ell\tilde{\hat{\mathbf{g}}}_\ell^H\tilde{\hat{\mathbf{g}}}_\ell+\bar{\hat{\mathbf{g}}}_\ell^H\bar{\hat{\mathbf{g}}}_\ell\bar{\hat{\mathbf{g}}}_\ell^H\bar{\hat{\mathbf{g}}}_\ell\right)\big\}. \tag{32}$$

Due to the space limit, we present the derivation of A_1, as

$$A_1\overset{(a)}{=}M(M+1)\gamma_{\hat{g}_\ell}^2+\mathbb{E}\{\tilde{\hat{\mathbf{g}}}_\ell^H\tilde{\hat{\mathbf{g}}}_\ell\bar{\hat{\mathbf{g}}}_\ell^H\tilde{\hat{\mathbf{g}}}_\ell\}+\mathbb{E}\{\tilde{\hat{\mathbf{g}}}_\ell^H\tilde{\hat{\mathbf{g}}}_\ell\tilde{\hat{\mathbf{g}}}_\ell^H\bar{\hat{\mathbf{g}}}_\ell\}+M^2\gamma_{\hat{g}_\ell}\lambda_\ell\Xi_{\ell,\ell}(\mathbf{\Theta})$$
$$\overset{(b)}{=}M(M+1)\gamma_{\hat{g}_\ell}^2+\sqrt{\lambda_\ell}\big[M^2\gamma_{\hat{g}_\ell}\sqrt{\lambda_\ell}\Xi_{\ell,\ell}(\mathbf{\Theta})+2\mathrm{Re}\left\{\bar{\mathbf{f}}_\ell^H\mathbf{\Theta}^H\bar{\mathbf{H}}_2\mathbf{e}_{\hat{\mathbf{g}}_\ell}\right\}\big]$$
$$\overset{(c)}{=}M(M+1)\gamma_{\hat{g}_\ell}^2+M^2\gamma_{\hat{g}_\ell}\lambda_\ell\Xi_{\ell,\ell}(\mathbf{\Theta}), \tag{33}$$

where we have exploited: in (a) [15, Lemma 2.9]; in (b) $\mathbb{E}\{\mathbf{x}^H\mathbf{y}\}=\mathbb{E}\{\mathrm{tr}(\mathbf{y}\mathbf{x}^H)\}$; in (c) $\mathbf{e}_{\hat{\mathbf{g}}_\ell}\triangleq\mathbb{E}\{\hat{\tilde{\mathbf{g}}}_\ell\hat{\tilde{\mathbf{g}}}_\ell^H\hat{\mathbf{g}}_\ell\}=\mathbf{0}_{M\times1}$. By using similar steps, we get

$$A_2=M\gamma_{\hat{g}_\ell}\lambda_\ell\Xi_{\ell,\ell}(\mathbf{\Theta}), \tag{34}$$
$$A3=M\gamma_{\hat{g}_\ell}\lambda_\ell\Xi_{\ell,\ell}(\mathbf{\Theta}), \tag{35}$$
$$A_4=M^2\lambda_\ell\Xi_{\ell,\ell}(\mathbf{\Theta})(\gamma_{\hat{g}_\ell}+\lambda_\ell\Xi_{\ell,\ell}(\mathbf{\Theta})). \tag{36}$$

To this end, by substituting (33)-(36), into (31) the desired result in (19) is obtained. □

References

[1] T. L. Marzetta, E. G. Larsson, H. Yang, and H. Q. Ngo, *Fundamentals of Massive MIMO*. Cambridge University Press, 2016.

[2] M. Matthaiou, O. Yurduseven, H. Q. Ngo, D. Morales-Jimenez, S. L. Cotton, and V. F. Fusco, "The road to 6G: Ten physical layer challenges for communications engineers," *IEEE Commun. Mag.*, vol. 59, no. 1, pp. 64–69, Jan. 2021.

[3] Q. Wu, S. Zhang, B. Zheng, C. You, and R. Zhang, "Intelligent reflecting surface-aided wireless communications: A tutorial," *IEEE Trans. Commun.*, vol. 69, no. 5, pp. 3313–3351, May 2021.

[4] K. Zhi, C. Pan, G. Zhou, H. Ren, M. Elkashlan, and R. Schober, "Is RIS-aided massive MIMO promising with ZF detectors and imperfect CSI?" *IEEE J. Sel. Areas Commun.*, vol. 40, no. 10, pp. 3010–3026, Oct. 2022.

[5] K. Zhi, C. Pan, H. Ren, and K. Wang, "Power scaling law analysis and phase shift optimization of RIS-aided massive MIMO systems with statistical CSI," *IEEE Trans. Commun.*, vol. 70, pp. 3558–3574, May 2022.

[6] K. Zhi *et al.*, "Two-timescale design for reconfigurable intelligent surface-aided massive MIMO systems with imperfect CSI," *arXiv preprint arXiv:2108.07622*, 2021.

[7] Q. Wu, X. Guan, and R. Zhang, "Intelligent reflecting surface-aided wireless energy and information transmission: An overview," *Proc. IEEE*, vol. 110, no. 1, pp. 150–170, Jan. 2022.

[8] C. Pan *et al.*, "Intelligent reflecting surface aided MIMO broadcasting for simultaneous wireless information and power transfer," *IEEE J. Sel. Areas Commun.*, vol. 38, no. 8, pp. 1719–1734, Aug. 2020.

[9] Q. Wu and R. Zhang, "Joint active and passive beamforming optimization for intelligent reflecting surface assisted SWIPT under QoS constraints," *IEEE J. Sel. Areas Commun.*, vol. 38, no. 8, pp. 1735–1748, Aug. 2020.

[10] D. Xu, V. Jamali, X. Yu, D. W. K. Ng, and R. Schober, "Optimal resource allocation design for large IRS-assisted SWIPT systems: A scalable optimization framework," *IEEE Trans. Commun.*, vol. 70, no. 2, pp. 1423–1441, Feb. 2022.

[11] E. Shi *et al.*, "Wireless energy transfer in RIS-aided cell-free massive MIMO systems: Opportunities and challenges," *IEEE Commun. Mag.*, vol. 60, no. 3, pp. 26–32, Mar. 2022.

[12] Z. Sun and Y. Jing, "On the performance of multi-antenna IRS-assisted NOMA networks with continuous and discrete IRS phase shifting," *IEEE Trans. Wireless Commun.*, vol. 21, no. 5, pp. 3012–3023, May 2022.

[13] Q. Wu and R. Zhang, "Intelligent reflecting surface enhanced wireless network via joint active and passive beamforming," *IEEE Trans. Wireless Commun.*, vol. 18, no. 11, pp. 5394–5409, Nov. 2019.

[14] S. M. Kay, *Fundamentals of statistical signal processing: Estimation theory*. Upper Saddle River, NJ, USA: Prentice-Hall, 1993.

[15] A. M. Tulino and S. Verdú, "Random matrix theory and wireless communications," *Found. Trends Commun. Inf. Theory*, vol. 1, no. 1, pp. 1–182, 2004.